ComEX

IEICE Communications Express, Vol.4, No.12, 387–392

Design of matching networks based on image impedances for near field MIMO

Kazuki Ishii[a)], **Naoki Honma, and Yoshitaka Tsunekawa**

Graduate School of Engineering, Iwate University,
4–3–5 Ueda, Morioka 020–8551, Japan
a) *t2314002@iwate-u.ac.jp*

Abstract: This paper proposes matching method based on image impedances for near field MIMO. In this letter, matching method, which can realize matching of all port at the same time by extending image impedances theory, is proposed. Numerical analysis and experimental results demonstrate the proposed matching method is effective in enhancing the channel capacity of the near field MIMO, where facing antennas strongly couple to each other.

Keywords: matching network, near field MIMO, conjugate image impedances

Classification: Antennas and Propagation

References

[1] J.-S. Jiang and M. A. Ingram, "Spherical-wave model for short-range MIMO," *IEEE Trans. Commun.*, vol. 53, no. 9, pp. 1534–1541, Sep. 2005. DOI: 10.1109/TCOMM.2005.852842

[2] N. Honma, K. Nishimori, T. Seki, and M. Mizoguchi, "Short range MIMO communication," Proc. 3rd EuCaP, pp. 1763–1767, Mar. 2009.

[3] D. Kwon, "Reactive near-field multiplexing and reliable diversity communication method," 2010 Proc. of the Fourth European Conference on Antennas and Propagation (EuCAP), 2010.

[4] M. A. Nikravan, D. Kwon, H. G. Schantz, and A. H. Unden, "Near-field MIMO communication utilizing both electric and magnetic field components," 2014 IEEE International Symposium on Antennas and Propagation and USNC-URSI Radio Science Meeting (AP-S 2014), pp. 474–475, Jul. 2014. DOI: 10.1109/APS.2014.6904568

[5] K. Shishido, K. Nishimori, and N. Honma, "Decoupling method for compact MIMO antenna utilizing MISO channel response on neighboring antennas," Proc. International Symposium on Antenna and Propagation (ISAP) 2011, Session FrP2-20, Oct. 2011.

[6] S. Roberts, "Conjugate-image impedances," *Proc. IRE*, vol. 34, pp. 198–204, Apr. 1946. DOI:10.1109/JRPROC.1946.234242

[7] N. Inagaki and S. Hori, "Fundamentals of wireless connections with near field coupled antennas," *IEICE Trans. Commun.*, vol. J94-B, no. 3, pp. 436–443, Mar. 2011.

[8] K. Ishii, N. Honma, and Y. Tsunekawa, "Matching method based on image impedances for near field MIMO," 2014 IEEE International Symposium on Antennas and Propagation and USNC-URSI Radio Science Meeting (AP-S 2014), vol. 3, pp. 1119–1120, Jul. 2014. DOI:10.1109/APS.2014.6904886

DOI: 10.1587/comex.2015XBL0150
Received October 30, 2015
Accepted November 24, 2015
Published December 22, 2015

[9] K. Ishii, N. Honma, and Y. Tsunekawa, "Experimental evaluation of matching method based on image impedances for near field MIMO," 2014 International Symposium on Antennas and Propagation (ISAP 2014), TH4C, pp. 411–412, Dec. 2014. DOI:10.1109/ISANP.2014.7026704
[10] U.-M. Jow and M. Ghovanloo, "Design and optimization of printed spiral coils for efficient transcutaneous inductive power transmission," *IEEE Trans. Biomed. Circuits Syst.*, vol. 1, no. 3, pp. 193–202, Sep. 2007. DOI:10.1109/TBCAS.2007.913130

1 Introduction

Recently, noncontact short range communication attracts attentions. Also, with the rapid spread of compact terminal including smartphone, high speed data transmission in short range is required.

A short range MIMO (Multiple-Input Multiple-Output) [1, 2] has been proposed for extending the data-rate of the short range wireless communication, where the channel capacity is enhanced by increasing the number of antennas at the transmitting and receiving antenna. When the distance between the transmitting and receiving array antennas is sufficiently short, the channel has low spatial correlation characteristics even with line-of-sight (LOS) situation. As a result, the short range MIMO offers a higher channel capacity than conventional MIMO does. In many studies, the short range MIMO has been evaluated at a high frequency band such as a millimeter wave band since larger bandwidth is available. However, the propagation loss is serious in such high frequency band.

The near field MIMO offers less propagation loss and high energy efficiency due to near field electromagnetic coupling since the distance between transmitting and receiving antennas is shorter than the wavelength [3, 4]. However, the impedances of the antennas are seriously affected by other antennas as well as their feed networks in the near field situation. Therefore, near field MIMO cannot use the conventional matching method based on only one side impedance of antenna. The feed networks for near field MIMO need to be designed iteratively since it is necessary to consider the effect of feed network, which is connected to the facing antenna [5]. Image impedance theory [6, 7] offers matching condition for SISO (Single-Input Single-Output) considering effect of other antennas. However, further extension of the theory is needed for near field MIMO.

In this letter, matching method, which can achieve matching of all port at the same time by using image impedances theory, are proposed [8, 9]. Numerical analysis and experimental results demonstrate the proposed matching method is effective in enhancing the channel capacity of near field MIMO. Also, it is found that the mutual coupling among the non-facing antennas does not affect the channel capacity, which has not been well considered in [9].

2 Matching method based on image impedance for near field MIMO

Fig. 1 shows equivalent circuit of 2×2 near field MIMO array. 2×2 near field MIMO array antenna system is treated as four port network. The signals transmitted

DOI: 10.1587/comex.2015XBL0150
Received October 30, 2015
Accepted November 24, 2015
Published December 22, 2015

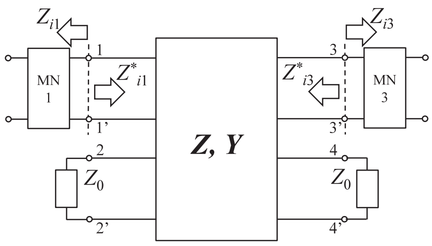

Fig. 1. The concept of the proposed method

from port 1 and 2 are received by port 3 and 4. In this figure, $\boldsymbol{Z}$ and $\boldsymbol{Y}$ represent impedance and admittance matrices of antenna system, respectively. Z_{i1} and Z_{i3} represent the image impedances for designing matching network (MN) of port 1 and 3, respectively. When we assume neighboring ports have a sufficiently low mutual coupling with the exception of two facing antenna ports, MNs can be designed using image impedance theory by focusing only on two facing antennas. For example, when port 2 and 4 are terminated by Z_0 represented reference for S-parameter, Z_{i1} and Z_{i3} are calculated by

$$Z_{i1} = \frac{1}{G_{11}(\theta_g + j\theta_b) - jB_{11}} \tag{1}$$

$$Z_{i3} = \frac{1}{G_{33}(\theta_g + j\theta_b) - jB_{33}} \tag{2}$$

where θ_g, θ_b are defined as

$$\theta_g = \sqrt{\left(1 + \frac{G_{13}^2}{G_{11}G_{33}}\right)\left(1 + \frac{B_{13}^2}{G_{11}G_{33}}\right)} \tag{3}$$

$$\theta_b = \frac{G_{13}B_{13}}{G_{11}B_{33}} \tag{4}$$

$$G_{pq} = \mathrm{Re}(Y_{pq}) \quad (p = 1, 2, 3, 4, \quad q = 1, 2, 3, 4) \tag{5}$$

$$B_{pq} = \mathrm{Im}(Y_{pq}) \quad (p = 1, 2, 3, 4, \quad q = 1, 2, 3, 4) \tag{6}$$

where Y_{pq} represents the element of $\boldsymbol{Y}$. When input and terminate impedances of port 1 and 3 are in the complex conjugate relation, matching can be achieved. Also the matching conditions for ports 2 and 4 can be determined in the same manner. Nevertheless, the MN design satisfying the above condition needs to be considered as follows.

As shown in Fig. 1, MNs for two facing coupled ports are designed by neglecting other two facing ports because the terminated non-facing ports little affect the matching condition due to small mutual coupling among them. When we focus on one certain antenna port, the observed reflection coefficient at the port is expressed as

$$\Gamma = \frac{Z_i^* - Z_0}{Z_i^* + Z_0} \tag{7}$$

where Z_i^* represent conjugate complex of the image impedance Z_i. The facing ports are assumed to be terminated by the image impedance element, and all other ports are terminated by Z_0. When the MN is designed using Γ, S-parameter of the MN is defined as

DOI: 10.1587/comex.2015XBL0150
Received October 30, 2015
Accepted November 24, 2015
Published December 22, 2015

IEICE Communications Express, Vol.4, No.12, 387–392

$$\boldsymbol{S}_M = \begin{pmatrix} S_{M11} & S_{M12} \\ S_{M21} & S_{M22} \end{pmatrix}. \tag{8}$$

The reflection coefficient through the MN becomes

$$S_{ref} = S_{M11} + S_{M12}(\Gamma^{-1} - S_{M22})^{-1}S_{M21} = 0. \tag{9}$$

Also, the design condition of MN is given by

$$S_{M22} = \Gamma^*. \tag{10}$$

Additionally, the lossless MN satisfies

$$\boldsymbol{S}_M \cdot \boldsymbol{S}_M^H = \boldsymbol{I} \tag{11}$$

where the operation, $\{\}^H$, is the complex conjugate transpose. From (9)~(11), S-parameter of MN is calculated by

$$S_{M22} = \Gamma^* \tag{12}$$

$$S_{M12} = \sqrt{1 - |S_{M22}|^2} e^{j\theta} \tag{13}$$

$$S_{M21} = S_{M12} \tag{14}$$

$$S_{M11} = -S_{M12}(\Gamma^{-1} - S_{M22})^{-1}S_{M21} \tag{15}$$

where θ is arbitrary value.

3 Simulation

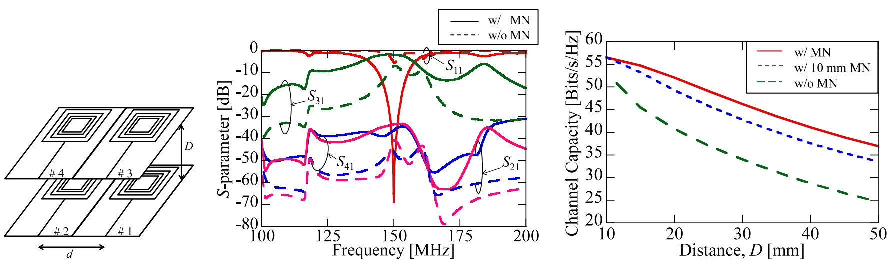

(a) Simulation Model (b) S-parameters (c) Channel Capacity

Fig. 2. Simulation results

Fig. 2(a) shows the antenna model in the simulation. An antenna system consists of four planar spiral antennas. This antenna element [10] is the square shaped spiral antenna printed on FR-4 substrate and the center frequency is set to 150 MHz. FR-4 substrate's relative dielectric constant is 4.4. In this figure, element spacing d is 65 mm, and distance between transmitting and receiving antennas is D. S-parameter of this model is analyzed by the method of moments. The signals transmitted from #1 and #2 are received by #3 and #4, respectively. Fig. 2(b) shows S-parameters of this model by the numerical analysis when D is 10 mm. In the figure, solid lines and broken lines represent the S-parameters with and without MNs respectively. The conjugate image impedances were

$$\begin{pmatrix} Z_{i1} & Z_{i2} \\ Z_{i3} & Z_{i4} \end{pmatrix} = \begin{pmatrix} 94.16 + j201.5 & 94.14 + j201.5 \\ 97.44 + j204.0 & 97.66 + j203.8 \end{pmatrix}, \tag{16}$$

DOI: 10.1587/comex.2015XBL0150
Received October 30, 2015
Accepted November 24, 2015
Published December 22, 2015

in this model. From this result, it can be seen that the proposed matching method improves S_{11} significantly and transmitting power S_{31} by 5 dB. Moreover, the mutual coupling, S_{21}, is even lower than transmission between facing antennas, S_{31}.

Fig. 2(c) plots the channel capacity versus distance between transmitting and receiving antennas. In this figure, solid line shows the channel capacity with the MN optimized for every distance, i.e. the MN is changed depending on D, dotted line shows the channel capacity with the MN designed only for $D = 10$ mm, and dashed line shows the channel capacity without MN. The transmitting power is set to 0 dBm, and noise power is −90 dBm. From this result, it can be seen the MN improves channel capacity by 12 bits/s/Hz at maximum since SNR (Signal to Noise Ratio) is improved thanks to the MNs at all port. Also, it is found that MN designed for 10 mm offers higher capacity than that without MN.

4 Experiment

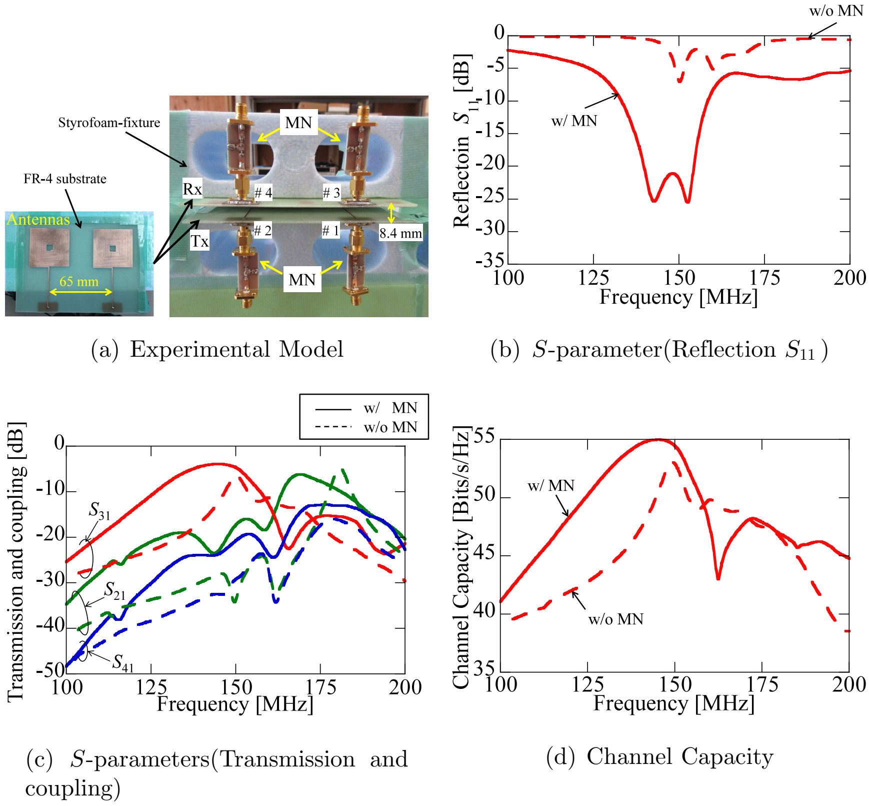

(a) Experimental Model

(b) S-parameter(Reflection S_{11})

(c) S-parameters(Transmission and coupling)

(d) Channel Capacity

Fig. 3. Experiment results

Fig. 3(a) shows the photos of fabricated antennas and MN based on the proposed matching method. Configuration of the antenna system and antenna element for experiment is same as condition of simulation. MNs were fabricated on FR-4 substrate, and consist of chip capacitors and inductors. The conjugate image impedances of all ports are calculated by using the measured S-parameter of the fabricated antennas. The calculated image impedances were

$$\begin{pmatrix} Z_{i1} & Z_{i2} \\ Z_{i3} & Z_{i4} \end{pmatrix} = \begin{pmatrix} 68.58 + j123.6 & 86.16 + j173.0 \\ 57.44 + j128.3 & 50.22 + j133.1 \end{pmatrix} \tag{17}$$

and the MNs were designed from this result.

DOI: 10.1587/comex.2015XBL0150
Received October 30, 2015
Accepted November 24, 2015
Published December 22, 2015

Fig. 3(b) shows that the frequency characteristics of the measured reflection characteristic S_{11} when D is 8.4 mm. In this result, reflection characteristics S_{11} are less than -10 dB at the center frequency when the MNs are used. Reflection characteristics of other ports are also improved.

Fig. 3(c) shows that the experimental result of transmission and coupling characteristics. This result indicates MN improves transmission, S_{31}. Moreover, the mutual coupling, S_{21}, is even lower than transmission, S_{31}, as with simulation results.

Fig. 3(d) plots the channel capacity versus frequency between transmitting and receiving antennas. The condition of calculating channel capacity is the same as that of the simulation. From this result, it is found the proposed MNs improve the channel capacity by 1.54 bits/s/Hz at the center frequency since reflection characteristics are improved.

5 Conclusion

This paper has proposed matching method based on image impedances suitable for near field MIMO. Simulations and experiments showed that the proposed matching method improves the channel capacity since reflection characteristics of all ports are improved at the same time. Both simulation and experiment results demonstrated that the proposed method is effective in enhancing channel capacity of near field MIMO.

Acknowledgments

This research was partially supported by JSPS KAKENHI (25709030).

DOI: 10.1587/comex.2015XBL0150
Received October 30, 2015
Accepted November 24, 2015
Published December 22, 2015